IL NUOVO CIMENTO **48 C** (2025) 65
DOI 10.1393/ncc/i2025-25065-6

Colloquia: IWM-EC 2024

Searching nuclear EoS from isospin transport in heavy-ion reactions around the Fermi energy domain

S. Mallik(1)(2), F. Gulminelli(3), D. Gruyer(3), C. Ciampi(4), J. Frankland(4), A. Chbihi(4), R. Bougault(3) and N. Le Neindre(3)

(1) *Physics Group, Variable Energy Cyclotron Centre - 1/AF Bidhan Nagar, Kolkata 700064, India*

(2) *Homi Bhabha National Institute, Training School Complex - Anushakti Nagar, Mumbai 400085, India*

(3) *Normandie Univ., ENSICAEN, UNICAEN, CNRS/IN2P3, LPC Caen - F-14000 Caen, France*

(4) *Grand Accelerateur National d'Ions Lourds (GANIL), CEA/DRF-CNRS/IN2P3 Boulevard Henri Becquerel, 14076 Caen, France*

received 26 November 2024

Summary. — The isospin transport of the quasi-projectile formed in the ^{64,58}Ni+^{64,58}Ni reactions around the Fermi energy domain is studied in the framework of the Boltzmann-Uehling-Uhlenbeck transport model. Isospin transport ratio is investigated, with the aim of ensuring an optimal comparison between experimental data and theoretical calculations and reducing the present uncertainties in the extraction of empirical equation of state parameters. We show that isospin transport ratio calculated from the neutron to proton ratio of the quasi-projectile as well as forward emitted free nucleons are not identical but both are sensitive to the symmetry energy at saturation, its slope and curvature. The sensitivity of the nuclear EoS to isospin transport ratios is greater for the quasi-projectile than for the free nucleon.

1. – Introduction

One of the most exciting challenges in modern nuclear physics and astrophysics is to understand the behavior of nuclear matter under extreme conditions. Heavy-ion reactions in the Fermi energy domain provide a unique opportunity to enrich our knowledge about the nuclear equation of state (EoS) at sub-saturation densities [1-3]. An interesting phenomenon in heavy-ion collisions is the differential transfer of protons and neutrons in binary reactions, named isospin diffusion. The degree of isospin equilibration led by isospin diffusion is known to be an excellent probe of the intricate dissipative reaction dynamics which is a competition of the mean-field and collision mechanism in the intermediate energy heavy ion reactions. The isospin diffusion is directly correlated to the density dependence of nuclear symmetry energy [4-8]. Isospin diffusion is measured by the isospin transport ratio, which can be defined as [4, 7, 9]

$$R = \frac{2x_{A_p+A_t} - x_{A_l+A_l} - x_{A_h+A_h}}{x_{A_l+A_l} - x_{A_h+A_h}}, \tag{1}$$

where, $x_{A_p+A_t}$ is an isospin sensitive observable which can be calculated for each reaction between projectile and target mass number A_p and A_t, respectively, corresponding to the same atomic number Z. Two different isotopes are used, and A_l (A_h) denotes the more neutron poor (rich).

The pioneering work by the MSU group at NSCL clearly identified that the isospin transport ratio is connected to the density dependence of the symmetry energy [7, 10]. However, tighter constraints could not be obtained mainly because of the uncertainty linked to the comparison protocol between nuclear experiments and transport simulations. In particular, the isotopic ratio of the quasi-projectile (QP) remnant was not directly experimentally measurable at that time. Surrogate variables were therefore employed, such as isoscaling parameters or light cluster isobaric ratios [7, 9, 11]. The aims of the present work are a) to investigate whether the isospin transport ratio calculated from two different isospin sensitive observables, namely i) $x = N/Z$ of the QP (which gives R_{QP}) and ii) $x = N/Z$ of the free nucleons forward emitted in the QP reference frame (which gives R_{free}), are identical or not and b) how they are sensitive to symmetry energy at saturation (E_{sym}), its slope (L_{sym}) and curvature (K_{sym}). In order to do that ^{58}Ni + ^{58}Ni, ^{64}Ni + ^{64}Ni, ^{58}Ni + ^{64}Ni and ^{64}Ni + ^{58}Ni reactions have been simulated for a wide range of impact parameter and projectile energy around the Fermi energy domain in the framework of isospin-dependent Boltzmann-Uehling-Uhlenbeck transport model (BUU@VECC-McGill) [12,13] with a metamodelling for the nuclear EoS [14]. The choice of the system and observables is due to the fact that these are being measured and analyzed by the INDRA-FAZIA Collaboration at GANIL [15, 16] with the future goal of reduction of the uncertainty of the empirical parameters and precise determination of nuclear EoS at sub-saturation densities.

The paper is structured as follows. In sect. **2**, a brief introduction of the transport model (BUU@VECC-McGill) is presented. The results are described in sect. **3**, and finally conclusion and future outlook are discussed in sect. **4**.

2. – Model description

Since we will focus on the properties of the positive rapidity region, the BUU@VECC-McGill transport model [12, 13, 17] calculations are performed in the projectile frame. Ground states of the projectile and target nuclei are constructed with a variational method [17-19] using Myers density profiles [20]. The ground state density distribution is then sampled using a Monte Carlo technique by choosing $N_{test} = 100$ test particles for each nucleon, with appropriate positions and momenta. The test particles of isospin $q = p, n$ move in a mean-field $U_q(\vec{r}, t)$ and will occasionally suffer two-body collisions, with probability determined by the isospin-dependent nucleon-nucleon scattering cross-section [21], provided the final state of the collision is not blocked by the Pauli principle. The mean field potential $U_q(\vec{r}, t) = U_q^{bulk}(\vec{r}, t) + U_q^{surf}(\vec{r}, t) + U_q^{coul}(\vec{r}, t)$, where $U_q^{bulk}(\vec{r}, t)$ represents the bulk part which is derived from the meta-functional [14] based on a polynomial expansion in density around saturation and including deviations from the parabolic isospin dependence through the effective mass splitting in the kinetic term and given by

(2)

$$U_q^{bulk}(\vec{r},t) =(v_0^{is}+v_0^{iv}\delta^2)+\sum_{k=1}^{4}\frac{k+1}{k!}(v_k^{is}+v_k^{iv}\delta^2)x^k+\frac{1}{3}\sum_{k=1}^{4}\frac{1}{(k-1)!}(v_k^{is}+v_k^{iv}\delta^2)x^{k-1}$$
$$+2\delta\tau_z(1-\delta\tau_z)\sum_{k=1}^{4}\frac{1}{k!}v_k^{iv}x^k+\exp\{-b(1+3x)\}\bigg[(a^{is}+a^{iv}\delta^2)\bigg\{\frac{5}{3}x^4$$
$$+(6-b)x^5-3bx^6\bigg\}+2\delta\tau_z(1-\delta\tau_z)a^{iv}x^5\bigg],$$

where $x=(\rho(\vec{r},t)-\rho_0)/3\rho_0$ and $\delta=(\rho_n(\vec{r},t)-\rho_p(\vec{r},t))/\rho(\vec{r},t)$. The parameters v_k^{is} with $k=1$ to 4 can be linked to the usual isoscalar empirical parameters of the saturation energy (E_{sat}), incompressibility modulus (K_{sat}), isospin symmetric skewness (Q_{sat}) and kurtosis (Z_{sat}), respectively, and v_k^{iv} with $k=1$ to 4 can be linked with the usual isovector empirical parameters of the symmetry energy (E_{sym}), slope (L_{sym}), and associated incompressibility (K_{sym}), skewness (Q_{sym}) and kurtosis (Z_{sym}), respectively. The effective mass of the nucleons also provides an effective momentum dependence, that is expected to correctly account for the mean-field nonlocality at the moderate energies around 30–60 MeV/nucleon considered in this paper. The finite range term $U_q^{surf}(\vec{r},t)=\frac{3C}{\rho_0^{2/3}}\nabla^2x$ [22] does not affect nuclear matter properties but produces realistic diffuse surfaces, and $U^{coul}(\vec{r},t)=\frac{1}{2}(1-\tau_q)U_c(\vec{r},t)$ is the standard Coulomb interaction potential with $\tau_q=-1$ (1) for protons (neutrons). The mean-field propagation is done by using the lattice Hamiltonian method which conserves energy and momentum very accurately [22]. Comparison of various observables from BUU@VECC-McGill model with other BUU and quantum molecular dynamics based models can be found in refs. [23-26].

For explaining the clustering phenomena in heavy-ion reactions, one needs an event-by-event computation in transport calculation, and mean-field fluctuations should be accounted for [27]. To do that, the computationally efficient prescription described in refs. [28, 29, 31] is followed. According to this prescription, the nucleon-nucleon collisions are computed at each time step with the physical isospin-dependent cross-section only among the A_p+A_t test-particles belonging to the same event. For each event, if a collision between two test particles i and j is allowed, the method proposed in refs. [27, 28] is followed: the $(N_{test}-1)$ test particles closest to i in configuration space are picked up, and the same momentum change $\Delta\vec{p}$ as ascribed to i is given to all of them. Similarly the $(N_{test}-1)$ test particles closest to j are selected and these are ascribed the same momentum change $-\Delta\vec{p}$ suffered by j. As a function of time this is continued till the event is over and the same procedure is repeated for each event. We consider free cross-section parameterized from experimental data. Finally to identify fragments, two test particles are considered as the part of the same cluster if the distance between them is less than or equal to 2 fm [29].

3. – Results

The ^{64,58}Ni + ^{64,58}Ni reactions are studied at projectile beam energy 52 MeV/nucleon from mid-central collision to very peripheral collision. For each reaction 500 events are

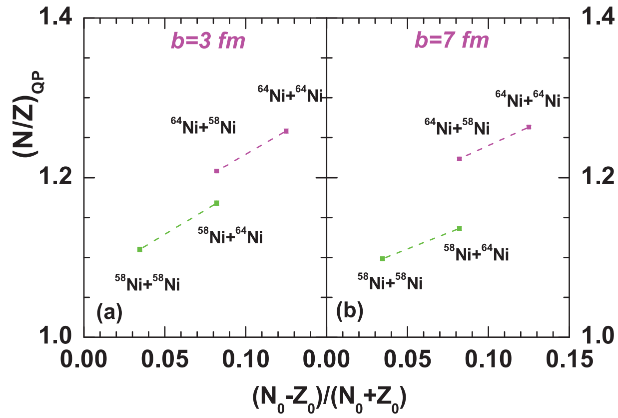

Fig. 1. – Neutron to proton ratio of QP as a function of $(N_0 - Z_0)/(N_0 + Z_0)$ for ^{58,64}Ni on ^{58,64}Ni reaction at 52 A MeV at an impact parameter $b = 3$ fm (left panel) and $b = 7$ fm (right panel). Green squares represent the result with ^{58}Ni projectile whereas magenta squares are for ^{64}Ni projectile. Dashed lines are drawn to guide the eyes. N_0 and Z_0 are the total number of neutrons and protons participating in the reaction.

simulated in the framework of BUU@VECC-McGill model with Sly5 EoS [30]. Calculations are performed in the projectile frame so the QP is identified from its momentum distribution peaked at a value close to zero. The freeze-out time of the QP is determined by studying the isotropy of momentum distribution [31] which is very close to unity for $t \geq 100$ fm/c. This freeze-out time is almost independent of the centrality of the reaction as well as projectile target combination.

The increased (decreased) value of neutron to proton ratio of the QP ($(N/Z)_{QP}$) formed in ^{58}Ni on ^{64}Ni (^{64}Ni on ^{58}Ni) reaction with respect to ^{58}Ni on ^{58}Ni (^{64}Ni on ^{64}Ni) reaction signals the isospin diffusion phenomenon, which tends to equilibrate the global N/Z ratio. This tendency is more effective at lower impact parameter due to increased overlap between the colliding nuclei. This is shown in fig. 1 at time $t = 300$ fm/c.

However, this neutron to proton ratio of the QP is sensitive to the secondary decay. It is customary in heavy-ion reactions to stop the dynamical evolution at the freeze-out time and to switch a statistical evaporation model [32, 33] for determining the cross-sections of final products. In this step, substantial error may arise due to i) uncertainty of precise coupling time and excitation and ii) inconsistency between the EoS used in the transport model and binding as well as level density used in the statistical evaporation model. To overcome this difficulty, the dynamical model is not coupled with statistical evaporation model and isospin transport ratio obtained from neutron to proton ratio of the QP as well as forward emitted free nucleons (in the projectile frame) is studied for a very long time (upto 500 fm/c) and it is observed that for $t \geq 150$ fm/c isospin transport ratio is almost independent of time [13]. Based on that, further studies on isospin transport ratio are done at $t = 300$ fm/c.

By construction, this isospin transport ratio R defined by eq. (1) is $+1$ and -1 for ^{64}Ni + ^{64}Ni and ^{58}Ni + ^{58}Ni reaction, respectively. For ^{58}Ni + ^{64}Ni and ^{64}Ni + ^{58}Ni reaction, $R = -1$ and $+1$, respectively, indicate no isospin equilibration whereas for both reactions R =0 represents full isospin equilibration, and values of R between 0 and -1 for ^{58}Ni + ^{64}Ni and between 0 and $+1$ for ^{64}Ni + ^{58}Ni reaction indicate the

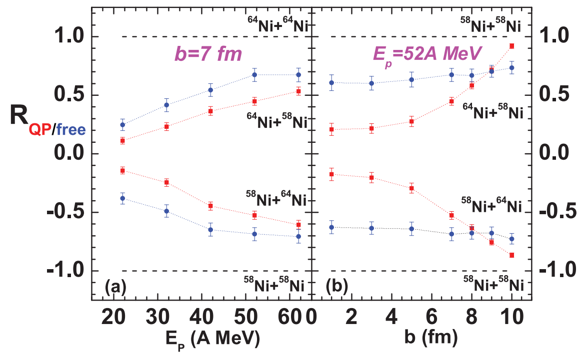

Fig. 2. – Projectile energy (left panel) and impact parameter (right panel) dependence of isospin transport ratio calculated from neutron to proton ratio of QP (red squares) and forward emitted free nucleons (blue circles) with time for ^{58,64}Ni on ^{58,64}Ni. Projectile energy (E_p) dependence is studied at constant impact parameter 7 fm whereas for centrality dependence projectile energy is fixed at 52 A MeV. Dashed lines are drawn to guide the eyes.

degree of equilibration which is connected to the nuclear EoS. Figure 2 represents the entrance channel effect on isospin diffusion from both N/Z of QP (R_{QP}) as well as that of free nucleons (R_{free}). Concerning R_{free}, in order to reduce the contribution of nucleons originated from the neck region, only particles with $p_z > 0\,\mathrm{MeV/c}$ in the QP frame are considered. The left panel shows the beam energy dependence at impact parameter $b = 7\,\mathrm{fm}$ whereas the right panel represents the impact parameter variation at beam energy 52 MeV/nucleon. The results clearly indicate that R_{QP} and R_{free} are different in general. With the increase of centrality of the reaction, participant region increases which enhances the degree of equilibration for isospin asymmetric reactions. Concerning the projectile energy dependence, the increase of absolute value of R for both observables reflects the shorter interaction time, increasing importance of nucleon-nucleon collisions and decreasing influence of the mean field, suggesting the importance of low energy experiments for precise measurements of the EoS properties. Recently, this is also experimentally verified by the first results from the same set of reactions performed by the INDRA-FAZIA Collaboration at GANIL [15].

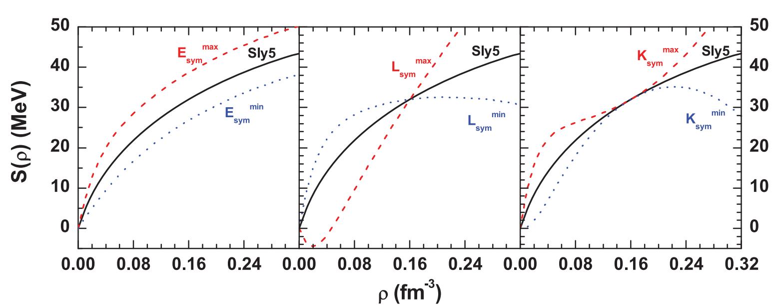

Fig. 3. – Density dependence of the symmetry energy for schematic EoS models obtained by independently varying E_{sym} (left panel), L_{sym} (middle panel) and K_{sym} (right panel), while the other parameters are taken from the Sly5 [30] EoS.

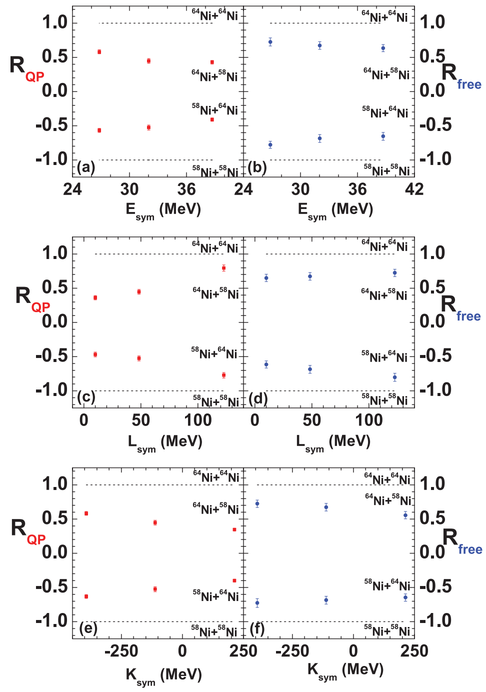

Fig. 4. – Sensitivity of isospin imbalance ratio calculated from neutron to proton ratio of QP (left panels) and free nucleons with $p_z c > 0\,\mathrm{MeV}$ (right panels) with E_{sym} (top panels), L_{sym} (middle panels) and K_{sym} (bottom panels) for ^{58,64}Ni on ^{58,64}Ni reaction with projectile beam energy 52 A MeV at impact parameter $b = 7\,\mathrm{fm}$.

In order to quantify the sensitivity of the isospin transport ratio to the density dependence of symmetry energy, the lowest order isovector parameters E_{sym}, L_{sym} and K_{sym} are tuned independently, *i.e.*, two of them are kept fixed at the reference of Sly5 EoS, whereas the third one is varied from a minimal to a maximal value compatible with the available empirical information (shown in fig. 3). The effect of tuning of these isovector parameters on isospin transport ratio for $^{58,64}\mathrm{Ni} + {}^{58,64}\mathrm{Ni}$ reactions at $b = 7\,\mathrm{fm}$ and $52\,\mathrm{MeV/nucleon}$ have been presented in fig. 4. In this energy domain, sub-saturation densities are probed and the symmetry energy reduces for lower value of E_{sym} and K_{sym} and higher values of L_{sym}. A lower symmetry energy leads to a decreased isospin transport, and higher absolute values of R. As a consequence, the magnitude of transport ratios increases (decreases) with increasing values of L_{sym} (E_{sym} and K_{sym}, respectively). Both R_{QP} and R_{free} are seen to vary by changing the symmetry energy parameters, but the dependence is much clearer when the QP is considered.

4. – Conclusion and future outlook

The isospin transport of the QP formed in the ^{64,58}Ni on ^{64,58}Ni reactions in the Fermi energy domain is investigated, using the BUU@VECC-McGill transport model with a metamodelling for the nuclear equation of state. It is observed that the isospin transport ratios obtained using the neutron to proton ratio of the projectile remnant, and that of forward-emitted free nucleons in the QP frame, are both sensitive to the density dependence of the symmetry energy. However, the absolute values of the isospin transport ratios obtained from two different observables are not identical. Sensitivity of nuclear EoS on isospin transport ratios of the QP is larger compared to the free nucleon. In order to reduce the error bar of nuclear EoS, transport calculation results with different realistic EoS are being compared with INDRA-FAZIA data of isospin transport ratio of the quasiprojectile. Isospin diffusion current densities are being calculated for estimating the precise region of sub-saturation densities responsible for isospin diffusion in heavy-ion reactions around the Fermi energy domain.

REFERENCES

[1] Li B. A., Chen L. W. and Ko C. M., *Phys. Rep.*, **464** (2008) 113.
[2] Li Bao-An and Schroder Wolf-Udo, *Isospin Physics in Heavy-Ion Collisions at Intermediate Energies* (Nova Science Pub. Inc.) 2001.
[3] Das Gupta S., Mallik S. and Chaudhuri G., *Heavy ion Reaction at Intermediate Energies: Theoretical Models* (World Scientific Publishers) 2019.
[4] Rami F. *et al.*, *Phys. Rev. Lett.*, **84** (2000) 1120.
[5] Shi L. and Danielewicz P., *Phys. Rev. C*, **68** (2003) 064604.
[6] Chen Lie-Wen, Ko Che Ming and Li Bao-An, *Phys. Rev. C*, **69** (2004) 054606.
[7] Tsang M. B. *et al.*, *Phys. Rev. Lett.*, **92** (2004) 062701.
[8] Johnston H., White T., Winger J., Rowland D., Hurst B., Gimeno-Nogues F., O'Kelly D. and Yennello S. J., *Phys. Lett. B*, **371** (1996) 186.
[9] Tsang M. B. *et al.*, *Phys. Rev. Lett.*, **102** (2009) 122701.
[10] Tsang M. B., Stone J. R., Camera F. *et al.*, *Phys. Rev. C*, **86** (2012) 015803.
[11] Zhang Y., Liu M., Xia C. J., Li Z. and Biswal S. K., *Phys. Rev. C*, **101** (2020) 034303.
[12] Mallik S., Chaudhuri G. and Gulminelli F., *Phys. Rev. C*, **100** (2019) 024611.
[13] Mallik S., Gulminelli F. and Gruyer D., *J. Phys. G: Nucl. Part. Phys*, **49** (2021) 015102.
[14] Margueron J., Casali R. and Gulminelli F., *Phys. Rev. C*, **97** (2018) 025805.
[15] Cimapi C. *et al.*, *Phys. Rev. C*, **106** (2022) 024603.
[16] Cimapi C. *et al.*, *Phys. Rev. C*, **108** (2023) 054611.
[17] Mallik S., Das Gupta S. and Chaudhuri G., *Phys. Rev. C*, **89** (2014) 044614.
[18] Lee S. J., Gan H. H., Cooper E. D. and Das Gupta S., *Phys. Rev. C*, **40** (1989) 2585.
[19] Cecil G. S. Das Gupta, and W. D. Myers, *Phys. Rev. C*, **22** (1980) 2018.
[20] Myers W. D., *Nucl. Phys. A*, **296** (1978) 177.
[21] Cugnon J., Hote D. L. and Vandermeulen J., *Nucl. Instrum. Methods B*, **111** (1996) 215.
[22] Lenk R. J. and Pandharipande V. R., *Phys. Rev. C*, **39** (1989) 2242.
[23] Walter H. *et al.*, *Prog. Part. Nucl. Phys.*, **125** (2022) 103962.
[24] Zhang Y. X. *et al.*, *Phys. Rev. C*, **97** (2018) 034625.
[25] Ono A. *et al.*, *Phys. Rev. C*, **100** (2019) 044617.
[26] Colonna M. *et al.*, *Phys. Rev. C*, **104** (2021) 024603.
[27] Bauer W., Bertsch G. F. and Das Gupta S., *Phys. Rev. Lett.*, **58** (1987) 863.
[28] Mallik S., Das Gupta S. and Chaudhuri G., *Phys. Rev. C*, **91** (2015) 034616
[29] Mallik S., Das Gupta S. and Chaudhuri G., *Phys. Rev. C*, **93** (2016) 041603(R).
[30] Chabanat E., Bonche P., Haensel P., Meyer J. and Schaeffer R., *Nucl. Phys. A*, **635** (1997) 231.
[31] Mallik S., Chaudhuri G. and Gulminelli F., *Phys. Rev. C*, **97** (2018) 024606.
[32] Camaiani A. *et al.*, *Phys. Rev. C*, **102** (2020) 044607.
[33] Mallik S., Chaudhuri G. and Das Gupta S., *Phys. Rev. C*, **91** (2015) 044614.